Cornell University, Ithaca, N. Y. 14850.
†Present address: Institut für Materialentwicklung, Kernforschungsanlage Jülich, D-517 Jülich, Germany.

[1]F. W. Young, Jr., T. O. Baldwin, and P. H. Dederichs, in *Vacancies and Interstitials in Metals*, edited by A. Seeger *et al.* (North Holland, Amsterdam, 1970).
[2]P. J. E. Aldred and M. Hart, Proc. Roy. Soc. London, Ser. A 332, 223 (1973).
[3]U. Bonse and G. Materlik, Z. Phys. 253, 232 (1972).
[4]J. A. Golovchenko, B. W. Batterman, and W. L. Brown, Phys. Rev. B 10, 4239 (1974).
[5]B. W. Batterman, Phys. Rev. 133, A759 (1964).
[6]B. W. Batterman, Phys. Rev. Lett. 22, 703 (1969).
[7]M. V. Laue, Ann. Phys. (Leipzig) 23, 705 (1935).
[8]The inverse of this statement is also true. The fluorescence measurement locates the electron-density Fourier component relative to the impurity. A previous knowledge of the impurity location in the lattice combined with the fluorescence measurement therefore determines the position (phase) of the Fourier component relative to the lattice. The knowledge of these phases for various Fourier components is required to experimentally reconstruct charge densities in the crystal. The phase of the Fourier component we use in this work is of course well known.
[9]M. Renninger, Z. Naturforsch. 16a, 1110 (1961).
[10]L. Kalsen, thesis, Institute of Physics, Aarhus University, 1976 (unpublished).
[11]T. N. Rodin and D. S. Y. Tong, Phys. Today 28, No. 10, 23 (1975); T. N. Rodin and D. L. Adams, in *Treatise in Solid State Chemistry*, edited by N. B. Hannay (Plenum, New York, 1976), Vol. 6, Chap. 5.

Raman-Active Lattice Vibrations of the Commensurate Superlattice in $2H$-$TaSe_2$ †

John A. Holy, Miles V. Klein, W. L. McMillan, and S. F. Meyer*
Department of Physics and Materials Research Laboratory, University of Illinois at Urbana-Champaign, Urbana, Illinois 61801
(Received 26 July 1976)

Raman spectra have been obtained on $2H$-$TaSe_2$ at room temperature and in the commensurate charge-density-wave, superlattice state. At low temperatures six new low frequency modes are seen having symmetries consistent only with a symmetric, three-charge-density wave. A microscopic model of the lattice dynamics of this state is fitted to the four strongest new Raman lines. These are assigned to amplitude and phase modes of the charge-density wave.

In many layered transition-metal dichalcogenides an electronic instability produces a charge-density wave (CDW), along with a periodic structural distortion (PSD) and a superlattice.[1-3] It has previously been shown that the CDW's strongly affect the Raman spectra of these materials.[4-6] This paper studies those new vibrations of the superlattice formed in $2H$-$TaSe_2$ that couple most strongly to the CDW. We first present Raman spectra from six new low-frequency zone-center phonons induced by the CDW. We then use these data with symmetry arguments to remove the ambiguities in the determination of the structure by electron[1] and neutron[2,3] diffraction. We finally present a microscopic model of the vibrations of the Ta ions about their new equilibrium sites.

The diffraction studies on $2H$-$TaSe_2$ show a transition from a normal lattice to one with an incommensurate CDW at 122 K (T_{NI}), followed at 90 K (T_{CI}) by a transition to a commensurate state.[2] Fairly strong evidence exists for a $3a_0 \times 3a_0 \times c_0$ unit cell in this state resulting from a superposition of three CDW's, but a single CDW with an $a_0 \times 3a_0 \times c_0$ unit cell cannot be completely ruled out. Moncton has determined the amplitudes and relative phases of the atomic displacements in the commensurate state, but the results are insensitive to the absolute phase,[3] which affects the point symmetry of the distorted structure and the Raman selection rules. We determine the phase from the observed selection rules and prove the existence of the three-CDW state.

Samples were grown by iodine-vapor transport.[7] They had a T_{NI} of 122 K and a T_{CI} of 110 K.[8] The high value of T_{CI} may be due to the low (30 ppm) level of transition-metal impurities. Raman measurements were made on a cleaved (0001) surface with use of a double grating monochromator equipped with a third monochromator and a 5145-Å laser beam. The incident and scattered beams made external angles of 75° and 0° with the c axis. Photon polarizations of hh (horizontal-horizontal) or vh (vertical-horizontal) relative to the scattering plane produced nearly pure xx or xy spectra. To verify assignments of symmetries, xz spectra were observed in a vh experiment from a $(1\bar{1}00)$ surface of a 1-mm-thick crystal. Cooling was provided by cold flowing helium gas. Temperatures were determined from the ratio of anti-Stokes to Stokes Raman intensities and are accu-

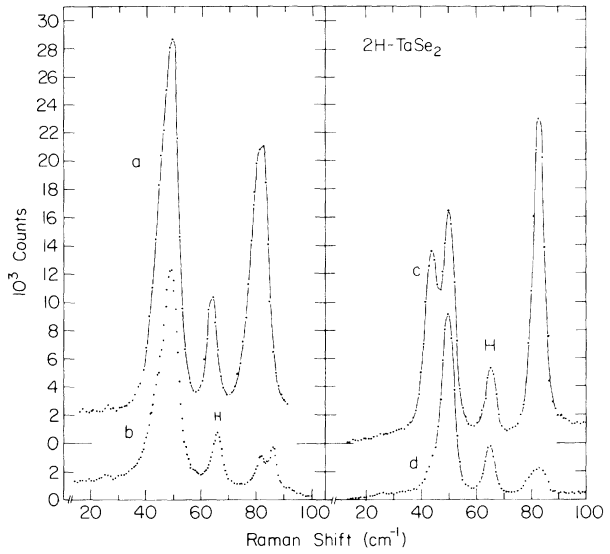

FIG. 1. Spectra of new Raman-active modes in the commensurate phase. Curve a: with hh geometry, T =35 K, resolution =2 cm^{-1}, 300 mW of laser power. Curve b: same as a, but with vh geometry. Curve c: with hh geometry, T =27 K, resolution =3 cm^{-1}, 250 mW of laser power. Curve d: same as c, but with vh geometry.

rate to about 20%.

At room temperature we observed the following Raman lines: E_{2g} at 22.5 and 207.5 cm^{-1}, A_{1g} at 234 cm^{-1}, and E_{1g} at 139 cm^{-1}. A very strong, broad band was observed at 148 cm^{-1}, which we assign to a combination of two LA phonons with wave vectors $\vec{q}$ of length $(0.4-1.0)q_M$ near the line $\Sigma(\Gamma M)$. The dispersion curve for this branch shows softening and a Kohn anomaly.[2]

As the sample is cooled through T_{NI}, the two-phonon band softens somewhat and weakens considerably. The strongest of the new features that appear are in the 40–100-cm^{-1} region and are shown in Fig. 1. They develop fully only in the commensurate phase and only at the lowest temperatures. Curves a and b reveal a weak E_{2g} doublet (xx and xy) at 82 and 86 cm^{-1}, a strong A_{1g} (xx only) line at 82 cm^{-1}, an E_{2g} line at 65 cm^{-1}, and a peak at 49 cm^{-1}. At 27 K the lowest peak splits into an A_{1g} line at 44 cm^{-1} and an E_{2g} line at 50 cm^{-1}. A comparison with the 2-K data of Smith, Tsang, and Shafer shows that no new features appear below 27 K.[4] No new E_{1g} lines were observed from 20–269 cm^{-1}.

In the CDW state, the PSD is primarily composed of lingitudinal displacements of Ta ions.[2,3] We write for the displacement of the ith Ta ion in the lth layer ($l=\pm 1$)

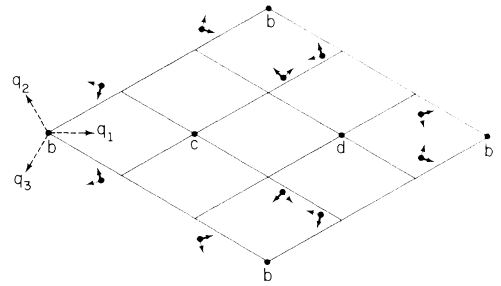

FIG. 2. Unit cell of the commensurate structure. Shown is the $z=c_0/4$ ($l=-1$) plane of Ta atoms. The labels b, c, and d are due to Wycoff as used in Ref. 9. The atoms displaced from the corners of the diamonds are at type-j sites. The magnitude of their displacements is greatly exaggerated. The Se atoms in the original $2H$ structure are equidistant above and below the midpoints of the right half of each small diamond.

$$\vec{u}_l(R_i) = \mathrm{Im}\sum_{j=1}^{3} (\vec{q}_j/q)\varphi_l{}^j \exp(i\vec{q}_i\cdot\vec{R}_i), \tag{1}$$

where $\varphi_l{}^j$ is the complex amplitude of the distortion. The vectors $\vec{q}_j$ are shown in Fig. 2 and have length $2q_M/3$. The primitive lattice sites at $\vec{R}_i$ are centers of inversion in the $D_{6h}{}^4$ space group of the original $2H$ lattice.[1,9] A symmetric three-CDW state will obey

$$\varphi_{-1}{}^1=\varphi_{-1}{}^2=\varphi_{-1}{}^3=\varphi_{-1}{}^{1*}=\varphi_{-1}{}^{2*}=\varphi_{-1}{}^{3*} \tag{2}$$

and for this structure, but not in general, it will belong to the old space group. It has even parity under the inversion operation.

The positions given by the dots in Fig. 2 are consistent with Moncton's results.[3] Assuming an inversion-symmetric three-CDW state he finds

$$\varphi_l{}^j = \epsilon a_0 e^{l(3.94i)}, \tag{3}$$

where a_0 = 3.44 Å and a lower bound for ϵ is 0.014. His measurements are insensitive to phase shifts which move the CDW's relative to the lattice and destroy the inversion symmetry.

Basis vectors for the new modes come from phonons in the old structure with wave vectors at new reciprocal lattice points. Six of these wave vectors belong to the star $\pm\vec{q}_j$ on the line Σ, and two belong to a star at the zone corner K: $\pm(\vec{q}_1-\vec{q}_2)$. The phonon coordinates generate reducible representations of $k=0$ phonons in the new space group. The reduction process is analogous to that in the "correlation method"[10]; the role of the site group is now played by the "small group of k."

We observe only a small set of the new modes

allowed by symmetry. The strongest apparently result from reduction of those phonons that show the Kohn anomaly, namely LA phonons on Σ. The symmetry of these phonons is that of longitudinal displacements of the Ta ions. The small group on Σ is C_{2v}, and these displacements for each of the two Ta ions in the old unit cell belong to representation A (or Σ_1). The correlation method gives

$$2A \text{ of } C_{2v} \rightarrow 2(A_{1g}+E_{2g}+B_{1u}+E_{1u}) \text{ of } D_{6h}. \quad (4)$$

The small group at K is D_{3h}. For each Ta atom, the displacements in the basal plane belong to representation E_2 (or K_6), yielding

$$2E_2 \text{ of } D_{3h} \rightarrow 2(E_{2g}+E_{1u}) \text{ of } D_{6h}. \quad (5)$$

The number of new Raman-active modes, $2A_{1g}+4E_{2g}$, is precisely what we observe below 100 cm^{-1} in Fig. 1.

In a single CDW state only two wave vectors, say $\pm\tilde{q}_1$, would contribute to the new $k=0$ modes, giving at most four new Raman-active modes. Thus we must have a three-CDW state. If inversion symmetry does not hold, the infrared-active E_{1u} modes will become simply E_1 modes and will be Raman active. No such modes were seen. Thus the state must be the fully symmetric one of Eqs. (1)–(3).

The weak E_{2g} doublet at 82 and 86 cm^{-1} is assigned to the contribution from the modes at K. The $2A_{1g}+2E_{2g}$ modes from Σ_1 phonons couple strongly to the CDW. They undergo large shifts and splittings, which we now describe via a low temperature microscopic model. The ionic displacements still obey Eq. (1) with time-dependent φ_l^j. The lattice kinetic energy is taken to be that of the Ta atoms with an effective mass of $M^*=206$ amu to account for the motion of the Se atoms.

The dominant contribution to the lattice potential energy from the electrons is due to the Peierls energy gap in the band structure. Let $W_l^j=\alpha|\varphi_l^j|$ denote one-half the energy gap for electrons in layer l with spanning wave vector $\tilde{q}_j$. α denotes the screened electron-phonon interaction. The electronic energy is approximately

$$E_{el}=-\sum_{jl}\int d^2x\, N(0)|W_l^j(x)|^2\ln|E_B/W_l^j(x)|^2, \quad (6)$$

where $N(0)$ is the density of states of electrons affected by the Peierls gap and E_B is an electronic bandwidth. We can then write for the lattice potential energy per unit volume

$$V=\tfrac{1}{2}N\sum_{l=\pm1}\{\Sigma_j[A|\varphi_l^j|^2-C|\varphi_l^j|^2\ln|\varphi_B/\varphi_l^j|^2-\mathrm{Re}(\tilde{B}\varphi_l^j)^3+F\,\mathrm{Re}(\varphi_l^j\varphi_{\bar{l}}^j)]$$
$$+D(|\varphi_l^1\varphi_l^2|^2+|\varphi_l^1\varphi_l^3|^2+|\varphi_l^2\varphi_l^3|^2)+\mathrm{Re}(\tilde{E}\varphi_l^1\varphi_l^2\varphi_l^3)\}, \quad (7)$$

where N is the density of Ta atoms. $\tilde{B}$ and $\tilde{E}$ are complex with moduli denoted by B and E. The third term is the lock-in energy, which is present only in the commensurate phase; the fourth term is the interlayer (Coulomb plus Van der Waals) interaction; and the fifth term results from competition of two CDW's for a common area of the Fermi surface. E and F are small. At zero temperature the static displacements are chosen to minimize the energy, and the CDW phases are dominated by the lock-in term. We expand about the symmetric solution of the form (2) and (3):

$$\varphi_l^j=\varphi_0 e^{il\theta}(1+a_l^j+ib_l^j). \quad (8)$$

The modulus φ_0 obeys

$$A-C\ln|\varphi_B/\varphi_0|^2+C-\tfrac{3}{2}B\varphi_0+2D\varphi_0^2+\tfrac{1}{2}\mathrm{Re}(\tilde{E}e^{i3\theta}\varphi_0)-F=0, \quad (9)$$

and a_l^j and b_l^j are small dynamic displacements of the amplitude and phase from equilibrium. We now expand the potential energy to second order in the a_l^j and b_l^j to find the dynamical matrix, whose eigenvalues give the phonon frequencies listed in Table I. The first four modes are amplitude modes; the A_{1g} mode (light arrows in Fig. 2) is assigned the highest energy. The second four are phase modes ("phasons")[11]; the A_{1g} mode (heavy arrows) has lowest energy.

The interlayer interaction provides a splitting of $4F$ between even- and odd-parity members of a pair of levels. This can be estimated roughly from the E_{2g} zone corner doublet or from the E_{2g} "interlayer" mode. We find that F is about 0.03 $eV/Å^2$. Other results from fitting to the four strong peaks are, in $eV/Å^2$, $B\varphi_0=0.053$, $E\varphi_0$

TABLE I. Normal modes of CDW.

Symmetry	ω_{obs} (cm^{-1})	$M^*\omega^2/4$
A_{1g}	82	$4C-3B\varphi_0+8D\varphi_0^2+E\varphi_0$
A_{1u}		$4C-3B\varphi_0+8D\varphi_0^2+E\varphi_0+4F$
E_{2g}	65	$4C-3B\varphi_0-4D\varphi_0^2-2E\varphi_0$
E_{1u}		$4C-3B\varphi_0-4D\varphi_0^2-2E\varphi_0+4F$
A_{1g}	44	$9B\varphi_0-3E\varphi_0$
A_{1u}		$9B\varphi_0-3E\varphi_0+4F$
E_{2g}	50	$9B\varphi_0$
E_{1u}		$9B\varphi_0+4F$

$=0.036$, $C=0.29$, $D\varphi_0^2=0.031$, and $A/C-\ln|\varphi_B/\varphi_0|^2=-0.90$.

Phase modes do not *a priori* have lower energy than amplitude modes, but we have made such an assignment in Table I, partly because of the temperature dependence of the modes. A satisfactory microscopic theory does not yet exist for T near T_{CI}, but those we have predict that the phase modes go soft at T_{CI}.[12] We have followed the modes in Fig. 1 to the vicinity of T_{CI}. The 65- and 82-cm^{-1} peaks weaken considerably but preserve their identity. The 44- and 50-cm^{-1} peaks merge and give a broad band at about 40 cm^{-1}. No modes go completely "soft," in agreement with the neutron data.[2] These results suggest that our lower-frequency modes are phase modes. This is supported by the calculation. Table I shows that the A_{1g}-E_{2g} splitting for the amplitude modes is $12\varphi_0^2+3E\varphi_0$, whereas the E_{2g}-A_{1g} splitting for the phase modes is $3E\varphi_0$. The D term in Eq. (7) is expected to be large and positive and the E term small. Thus the higher frequency A_{1g}, E_{2g} pair, which shows the larger splitting, is probably a pair of amplitude modes.

We thank D. E. Moncton for discussing his neutron measurements.

†Work supported by the Advanced Research Projects Agency (monitored by U. S. Air Force Office at Scientific Research under Contract No. F44620-75-C-0091) and by U. S. Energy Research and Development Administration Contract No. E(11-1)-1198.

*Present address: Lawrence Livermore Laboratory, Livermore, Calif. 94551.

[1]J. A. Wilson, F. J. Di Salvo, and S. Mahajan, Adv. Phys. 24, 117 (1975).

[2]D. E. Moncton, J. D. Axe, and F. J. Di Salvo, Phys. Rev. Lett. 34, 734 (1975).

[3]D. E. Moncton, Ph.D. thesis, Massachusetts Institute of Technology, 1975 (unpublished).

[4]J. E. Smith, Jr., J. C. Tsang, and M. W. Shafer, Solid State Commun. 19, 283 (1976).

[5]J. R. Duffey, R. D. Kirby, and R. V. Coleman, Bull. Am. Phys. Soc. 21, 260 (1976).

[6]M. V. Klein, J. A. Holy, and S. F. Meyer, Bull. Am. Phys. Soc. 21, 338 (1976).

[7]H. Schäfer, *Chemical Transport Reactions* (Academic, New York, 1964).

[8]R. A. Craven, unpublished.

[9]*International Tables for X-ray Crystallography*, edited by N. F. M. Henry and K. Lonsdale (Kynoch Press, Birmingham, 1965), Vol. 1.

[10]H. Winston and R. S. Halford, J. Chem. Phys. 17, 607 (1949).

[11]A. W. Overhauser, Phys. Rev. B 3, 3173 (1971).

[12]P. A. Lee, T. M. Rice, and P. W. Anderson, Solid State Commun. 14, 703 (1974).

rf-Induced Potential inside a Superconducting Weak Link*

Ming L. Yu
Brookhaven National Laboratory, Upton, New York 11973

and

J. E. Mercereau
California Institute of Technology, Pasadena, California 91125

(Received 10 September 1976)

Voltage measurements made inside a superconducting weak link suggest that under ac conditions a nonequilibrium quasiparticle current exists and stimulates a quasiparticle potential.

The superconducting weak link has many of the quantum interference aspects of a Josephson tunnel junction and has often been treated as a Josephson tunnel junction coupled with reactive and dissipative circuit elements. However the electron physics underlying weak-link phenomena and conducting barriers is probably much more complex than that of Josephson tunneling through in-